Investigations on the Effect of Mn Ions on the Local Structure and Photocatalytic Activity of Cu(I)−ZSM-5 Catalysts

Haijun Chen,[†] Masaya Matsuoka,[†] Jinlong Zhang,[‡] and Masakazu Anpo*[,†]

Department of Applied Chemistry, Graduate School of Engineering, Osaka Prefecture University, 1-1 Gakuen-cho, Sakai, Osaka 599-8531, Japan, and Institute of Fine Chemicals, East China University of Science and Technology, 130 Meilong Road, Shanghai 200237, P. R. China

Received: October 1, 2005; In Final Form: January 11, 2006

The introduction of Mn ions into Cu(I)-ZSM-5 was found to lead to an enhancement of the photocatalytic activity for the direct decomposition of N_2O into N_2 and O_2 at 298 K. Various in-situ techniques such as ESR, photoluminescence, XAFS as well as a combination of CO−FT-IR and CO−TPD measurements revealed that the accommodation of Mn ions within ZSM-5 zeolite cavities significantly affects the location sites of the ion-exchanged Cu(II) ions as well as the local structure of the Cu(I) ion species formed by evacuation at high temperatures. Moreover, the introduction of Mn ions into ZSM-5 led to an increase in the amount of 3-coordinated Cu(I) species at the main channel of the zeolite, playing a major role as the active species for the photocatalytic decomposition of N_2O into N_2 and O_2.

Introduction

Nitrogen oxides (NO_x) released from vehicle engines and industrial boilers have long been a major cause of air pollution. One of the most desired approaches for NO_x abatement would be the direct decomposition of NO_x into N_2 and O_2. Initially, overexchanged Cu−ZSM-5 was thought to be a highly active catalyst for such a direct decomposition reaction[1] and, in fact, it has been reported that Cu(I)−ZSM-5 acts as an effective photocatalyst for the direct decomposition of NO_x (NO, N_2O) into N_2 and O_2 under UV light irradiation.[2−10] Subsequent studies have focused on improving the catalytic performance of Cu ion-exchanged zeolites, such as Cu−ZSM-5 and Cu−Y, for the decomposition of NO_x by the additional exchange of other metal ions into these zeolites. Iwamoto et al.[11] have found that the exchange of Ni and Co could induce increased catalytic performance of Cu−Y. Studies have also been carried out on introducing rare-earth elements into the zeolites with good results. For example, the addition of cerium,[12,13] lanthanum,[14] or samarium[15] has been shown to increase the catalytic activity of Cu−ZSM-5. A study on the effect of metal ions on Cu−ZSM-5 by Zhang et al.[16] reports that the cerium ions hindered the sintering of the catalytically active components. Budi et al.[13] and Kucherov et al.[14] have interpreted this promotion behavior in terms of the changes in the chemical bonding between the isolated Cu(II) cations and the framework oxygen of ZSM-5, linked in turn, to the Al(III) ions. Centi and Perathoner et al.[17] have suggested some factors such as the modification of the electrostatic field and the surface potential within the pores/cavities of the zeolite, i.e., changes in the local "softness" around the Cu ions and the diffusion properties of NO. Parvulescu et al.[15,18] have proposed that the second metal contributes to locating and stabilizing the Cu ions at the active sites. However, although the results of the reactions are of significance in understanding the catalysts, there are yet few studies showing direct evidence to confirm the mechanisms behind the reactions.

This work deals with the incorporation of Mn ions into Cu−ZSM-5, which led to the effective enhancement of the photocatalytic activity of Cu(I)−ZSM-5 for the direct decomposition of N_2O into N_2 and O_2 at 298 K. Detailed characterizations of the local structure as well as the photoexcited states of the Cu ions and investigations into the effects of the Mn cations have been carried out by various in-situ molecular spectroscopic techniques such as ESR, photoluminescence, XAFS and a combination of in-situ CO−FT-IR and CO−TPD. The introduction of Mn ions into the Cu−ZSM-5 zeolite was confirmed to significantly affect the location sites of the ion-exchanged Cu(II) ions as well as the local structure of the Cu(I) ion species produced by evacuation treatment at high temperatures, thus, leading to an enhancement of the photocatalytic activity of Cu(I)−ZSM-5.

Experimental Section

The H−ZSM-5 zeolite was prepared by calcination of the NH_4−ZSM-5 zeolite ($SiO_2/Al_2O_3 = 39$, Tosoh Corp.) in air at 773 K for 5 h. A 1 g sample of H−ZSM-5 was suspended in 100 mL of $Mn(NO_3)_2$ solution and stirred for 24 h at room temperature. The obtained solid was recovered by centrifugation, washed with distilled water, then dried in air at 373 K for 24 h to obtain Mn−ZSM-5. After calcination in air at 773 K for 3 h, the prepared Mn−ZSM-5 was further ion-exchanged with 100 mL of a $Cu(NO_3)_2$ solution for 24 h at room temperature followed by centrifuging, washing, and drying in air at 373 K for 24 h. These samples were referred to as Cu(II)Mn−ZSM-5 and, as reference, Cu(II)−ZSM-5 was also prepared by ion-exchange of H−ZSM-5 with $Cu(NO_3)_2$ solution following the same preparation procedures as for Mn−ZSM-5. The contents of the Cu and Mn ions in the obtained samples were determined as metals by atomic absorption flame emission spectrophotometry (Shimadzu AA-6400F). The chemical compositions of typical solutions for ion-exchange and the prepared samples are summarized in Table 1. The total ion-exchange degree of Cu-

* Corresponding author. Fax: +81-72-254-9910 E-mail: anpo@chem.osakafu-u.ac.jp.
[†] Osaka Prefecture University.
[‡] East China University of Science and Technology.

10.1021/jp055604+ CCC: $33.50
Published on Web 02/09/2006

TABLE 1: Chemical Composition of the Solutions for Ion-Exchange Treatment and the Ion-Exchanged Samples

	concentrations of the solutions for ion-exchange treatment (M)		metal loadings of the ion-exchanged samples (wt %)		degree of ion-exchange (%)	
samples	$Cu(NO_3)_2$	$Mn(NO_3)_2$	Cu	Mn	Cu	Mn
Cu(II)−ZSM-5	0.017		1.27		49.1	
Mn−ZSM-5		0.035		0.10		4.5
Cu(II)Mn−ZSM-5	0.029	0.035	1.22	0.09	47.2	4.1

(II)−ZSM-5 and Cu(II)Mn−ZSM-5 were comparative at around 50%, as shown in Table 1.

All the quartz cells used for the in-situ spectroscopic measurements were specially designed to be connected to a vacuum line for thermal treatment of the samples with a well-controlled gas dosage. The UV−vis spectra were recorded using a double-beam digital spectrophotometer (Shimadu UV-2200A) with $BaSO_4$ powder as reference. The ESR spectra were recorded at 77 K with a JES−RE2X spectrometer operating in the X-band mode. The magnetic field was calibrated with respect to the standard DPPH (2,2-diphenyl-1-picrylhydrazyl hydrate) signal. Prior to spectroscopic measurements and photocatalytic reactions, the Cu(II) ion samples, Cu(II)−ZSM-5 and Cu(II)-Mn−ZSM-5, were evacuated at the desired temperatures where almost all of the Cu(II) ions were reduced to Cu(I) ions selectively through the autoreduction of Cu(II).

The photoluminescence spectra were recorded at both 77 and 298 K with a Spex Fluorolog II spectrofluorometer equipped with a Xenon UV−vis−near-IR excitation lamp at an excitation wavelength of 280 nm. Cu K-edge XAFS (XANES and EXAFS) measurements were measured under a ring operating condition of 2.5 GeV at the BL-10B beam line facility of the High Energy Accelerator Research Organization, KEK, in Tsukuba, Japan. The X-rays were monochromized through a double-crystal monochromator of Si(311) and the spectra were recorded in the transmission mode in an ionization chamber fitted with N_2-(I_0) and N_2/Ar(I). The photon energy was calibrated by a characteristic preedge peak in the spectrum of copper foil. Curve fitting analysis of the EXAFS spectra was conducted by applying the $k^3\chi(k)$ function in κ-space ($3 < k < 9$ Å^{-1}) with a REX 2000J program (Rigaku).

The FT-IR spectra were recorded with an FT-IR spectrometer (JASCO FT-IR 7300) using a TGS detector under a nominal resolution of 2 cm^{-1} and by averaging 100 scans in transmission mode. CO−TPD experiments were carried out on the samples (50 mg) within a quartz cell. The samples were sufficiently exposed to CO gas until adequate adsorptions of CO were reached, followed by evacuation at 298 K for 30 min in order to remove the physically absorbed CO molecules. CO−TPD experiments were then carried out in a temperature range from 323 to 873 K with a heating rate of 5 K/min. The effluents were then analyzed using a quadrupole mass spectrometer (M-QA100TS, Anelva). The photocatalytic decomposition reactions of N_2O were carried out under UV irradiation of the Cu(I) ion catalysts (50 mg) in the presence of N_2O (10 Torr) with a 500 W high-pressure mercury lamp (USH-500BY, $\lambda > 200$ nm) through a water filter at 298 K. A UV-25 filter (Toshiba, $\lambda > 250$ nm) was used to examine the effect of the irradiation wavelength on the reaction.

Results and Discussions

ESR Investigations on the Local Structure of the Cu(II) Species within the Cu(II) Ion Samples and Their Reduction Processes. ESR measurements were performed to investigate the local structures as well as the reduction processes of the paramagnetic Cu(II) ions within Cu(II)Mn−ZSM-5 and Cu(II)−ZSM-5. The as-synthesized Cu(II) ion samples exhibited broad and structureless ESR spectra due to the hydrated hexa-coordinated Cu(II) ions (not shown). After evacuation at high temperatures, most of the adsorbed molecules such as H_2O were removed and the resolution of four characteristic hyperfine structures attributed to the nucleus of the copper ($I = 3/2$) were observed, as shown in Figure 1. Two copper moieties with different spin-Hamiltonian parameters, $Cu(II)_\alpha$ and $Cu(II)_\beta$, could be observed for the Cu(II)Mn−ZSM-5 and Cu(II)-ZSM-5 evacuated above 673 K. The spin-Hamiltonian parameters observed for the $Cu(II)_\alpha$ and $Cu(II)_\beta$ species showed good agreement with those reported for Cu(II) ions with a square-pyramidal coordination at the M7 sites (i.e., ion-exchange sites close to the wall in the main channel) and Cu(II) ions with a distorted square-pyramidal coordination at the Z5 sites (i.e., ion-exchange sites in zigzag channels) of the ZSM-5, respectively.[19,20] (Definitions of the individual Cu sites and their locations in the ZSM-5 framework are shown in Figure S1, Supporting Information.) It was also clearly seen that the ratio of the $Cu(II)_\alpha$ against the $Cu(II)_\beta$ species was larger for Cu(II)Mn−ZSM-5 than for Cu(II)−ZSM-5. These results suggest that pre-ion-exchanged Mn ions preferentially occupy the Z5 sites and induce more Cu(II) ions to be exchanged at the six-membered rings in the main channels (M7 sites) to form a square pyramidal coordination ($g_{||} = 2.34$, $A_{||} = 155$ G), while fewer Cu(II) ions located in the zigzag channels (Z5 sites) lead to a distorted square pyramidal coordination ($g_{||} = 2.31$, $A_{||} = 168$ G).

Further evacuation of Cu(II)Mn−ZSM-5 at temperatures above 673 K led to a drastic decrease in the intensity of the ESR signals, accompanied by minor changes in their spectral parameters and line shapes, indicating the reduction of the Cu(II) species. In fact, the Cu(I) ion catalysts evacuated at temperatures above 873 K showed a typical photoluminescence of the Cu(I) species under UV light irradiation, as shown in Figure 2, indicating that the Cu(II) species are reduced to the Cu(I) species. Detailed assignments of the observed photolu-

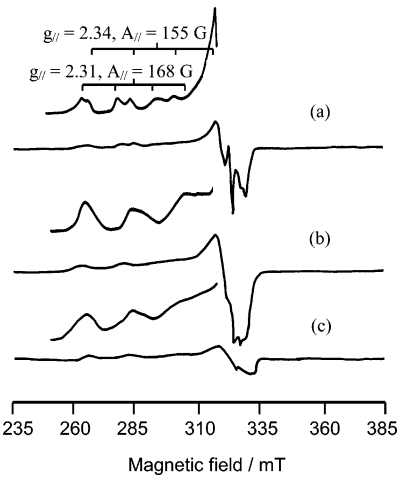

Figure 1. ESR spectra of (a) Cu(II)−ZSM-5; and (b, c) Cu(II)Mn−ZSM-5 evacuated at various temperatures for 1 h. Evacuation temperatures: (a) 873 K; (b) 673 K; and (c) 873 K.

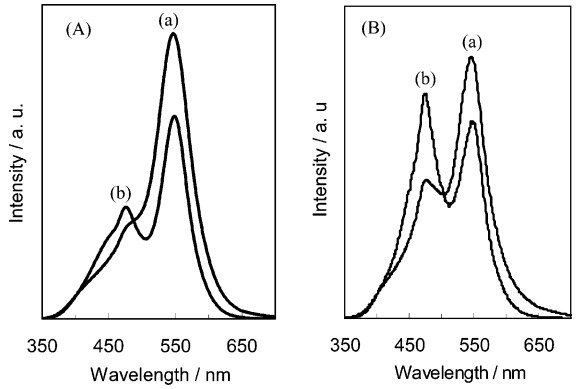

Figure 2. The observed photoluminescence spectra measured at (A) RT and (B) 77 K of (a) Cu(I)Mn−ZSM-5 and (b) Cu(I)−ZSM-5 prepared by the evacuation of the as-prepared samples at various temperatures for 1 h. Evacuation temperature: (a) 973 K; (b) 1173 K.

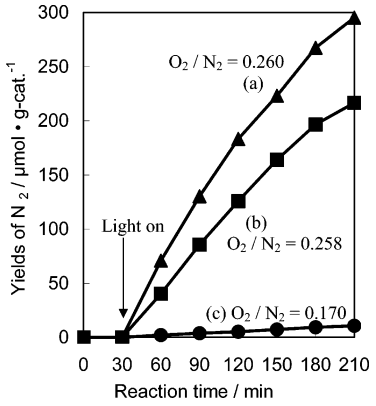

Figure 3. Time profiles of the photocatalytic decomposition reaction of N_2O into N_2 and O_2 at 298 K on (a) Cu(I)Mn−ZSM-5; (b) Cu(I)−ZSM-5; and (c) Mn−ZSM-5 prepared by the evacuation of the as-prepared samples at various temperatures for 1 h. Evacuation temperature: (a) 973 K; (b) 1173 K; and (c) 973 K.

minescence will be discussed further. The reduction mechanism of Cu(II) into Cu(I) can be proposed as follows:

$$2Cu^{2+} + H_2O \rightarrow 2Cu^{+} + 2H^{+}\,(\text{Brönsted acid}) + 1/2O_2$$

The prepared Cu(I)Mn−ZSM-5 and Cu(I)−ZSM-5 catalysts were found to exhibit photocatalytic activity for N_2O decomposition into N_2 and O_2.

Photocatalytic Activities of the Cu(I)Mn−ZSM-5 and Cu(I)−ZSM-5 Catalysts. The reaction time profiles of the photocatalytic decomposition of N_2O into N_2 and O_2 at 298 K on Cu(I)Mn−ZSM-5, Cu(I)−ZSM-5, and Mn−ZSM-5 are shown in Figure 3. UV light irradiation of Cu(I)Mn−ZSM-5 and Cu(I)−ZSM-5 in the presence of N_2O at 298 K led to the efficient formation of N_2 and O_2, while the activity of Mn−ZSM-5 was much lower than that of Cu(I)Mn−ZSM-5 and Cu(I)−ZSM-5. Under dark conditions, no reaction was observed to proceed, indicating that these reactions were photocatalytic. Cu(I)Mn−ZSM-5 catalysts with different loadings of Mn ions were prepared by changing the concentrations of the solutions of $Mn(NO_3)_2$ used for ion-exchange treatment. All the Cu(I)-Mn−ZSM-5 catalysts showed higher activity than Cu−ZSM-5, as shown in Figure 3 and Table 2, while the Cu(I)Mn−ZSM-5 containing about 0.1 wt. % Mn ions showed the highest activity among these catalysts. CuMn−ZSM5 containing 1.22 wt. % Cu and 0.1 wt. % Mn ions was, thus, selected for further spectroscopic characterizations.

TABLE 2: Photocatalytic Activity[a] of Cu(I)Mn−ZSM5 for the Decomposition of N_2O into N_2 and O_2

sample number	metal loadings (wt %)		yields of N_2 (mmol/mol Cu)	yields of O_2 (mmol/mol Cu)
	Cu	Mn		
1	1.27	0	1082.87	278.85
2	1.14	0.05	1232.34	309.93
3	1.22	0.10	1536.91	400.57
4	1.34	0.13	1230.60	283.25
5	1.06	0.18	1267.43	249.99

[a] Photocatalytic reactions were carried out for 3 h. The activities were evaluated as the yields of N_2 per mol Cu atoms and the Cu ions were considered to be the main active species for the photocatalytic decomposition of N_2O while Mn−ZSM5 showed poor activity.

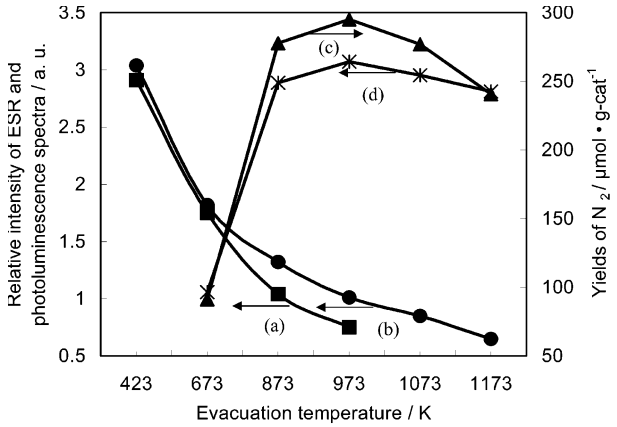

Figure 4. Effect of the evacuation temperature on the relative intensity of the ESR spectra of (a) Cu(II)Mn−ZSM-5; and (b) Cu(II)−ZSM-5 due to Cu(II) ions; (c) the yields of N_2 for the photocatalytic decomposition of N_2O at 298 K for 3 h; and (d) the relative yields of the photoluminescence due to Cu(I) ions measured at 298 K.

Figure 4a shows the effect of the evacuation temperature of Cu(II)Mn−ZSM-5 on the intensity of the ESR spectra assigned to Cu(II). With an increase in the evacuation temperature, the intensity of the ESR spectrum due to the Cu(II) ions decreased and the color of the sample changed from light blue to white, indicating that the evacuation of Cu(II)Mn−ZSM-5 led to a reduction of the Cu(II) ions into Cu(I). It was also found that the intensity of the photoluminescence due to the Cu(I) ions measured at 298 K increased with an increase in the degassing temperature of the original Cu(II)Mn−ZSM-5 sample, passing through a maximum at 973 K and then decreasing at higher evacuation temperatures, as shown in Figure 4d. The photocatalytic activity of Cu(I)Mn−ZSM-5 shows a good parallel relationship with the intensity of the photoluminescence due to the Cu(I) ions, suggesting that they play an important role as the active species in this reaction.

The Cu(II) ions exchanged within Cu(II)Mn−ZSM-5 seems to be more easily reduced than those within Cu(II)−ZSM-5, as shown in Figure 4, since the intensity of the ESR spectrum of Cu(II)Mn−ZSM-5 (Figure 4a) decreases more remarkably at temperatures above 873 K than for Cu(II)−ZSM-5, as shown in Figure 4b. In fact, Cu(I)Mn−ZSM-5 prepared by evacuation at 973 K exhibited the highest photocatalytic activity (Figure 4c) while for Cu(I)−ZSM-5, evacuation at 1173 K led to photocatalytic activity.[10]

ESR measurements were also employed to investigate the oxidation states of the Mn ions in the ZSM-5 zeolites. The ESR spectrum of Mn−ZSM-5 evacuated at 423 K for 1 h showed six hyperfine lines with spin-Hamiltonian parameters of $g = 2.0$ and $A = 83$ G, which is consistent with the reported parameters for Mn(II) ions having a distorted octahedral

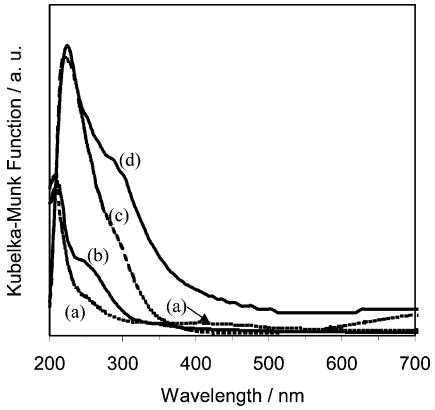

Figure 5. UV−vis spectra of (a, b) Mn−ZSM5; (c) Cu(I)−ZSM-5; and (d) Cu(I)Mn−ZSM-5 prepared by the evacuation of the samples at various temperatures for 1 h. Evacuation temperature: (a, d) 973 K; (b) 473 K; (c) 1173 K.

symmetry.[21−23] The UV−vis spectra of Mn−ZSM-5, Cu(I)−ZSM-5 and Cu(I)Mn−ZSM-5 are shown in Figure 5. Evacuation of Mn−ZSM5 at high temperatures led to a decrease in the absorption band at around 250 nm due to the Mn(II) ions[25] as well as to a broad absorption band at 350−500 nm due to the Mn(III) and Mn(IV) ions.[24] These results suggest that Mn(II) is oxidized into Mn(III) and Mn(IV) by evacuation treatment at high temperatures. Based on these results, the oxidation of the Mn(II) ions to Mn(III) and Mn(IV) was seen to facilitate the reduction of Cu(II) ions into Cu(I) in Cu(I)Mn−ZSM-5, despite a report of an autoreduction of Cu(II) ions into Cu(I) in Cu−ZSM-5 under evacuation at high temperatures from 673 to 1173 K.[10] Cu(I)Mn−ZSM-5 and Cu(I)−ZSM-5 show a main absorption band in wavelength regions from 230 to 320 nm, which has been assigned to the $(3d^{10})^1S_0 \rightarrow (3d^9 4s^1)^1D_2$ transition of the Cu(I) ions.[25] It is clear that Cu(I)Mn−ZSM-5 shows a much stronger absorption band in wavelength regions above 250 nm as compared to Cu(I)−ZSM-5.

Local Structure of Cu(I) Ions within the Cu(I)Mn−ZSM-5 and Cu(I)−ZSM-5 Catalysts. *XAFS Investigations.* The XANES spectra can provide direct information on the oxidation state of the copper species,[26−29] and it is known that a well-defined preedge peak at 8982−8984 eV is assigned to the dipole-allowed $1s \rightarrow 4p_{xy}$ electronic transition of two-coordinate Cu(I) ions along the *z*-axis, or the $1s \rightarrow 4p_x$ electronic transition of three-coordinate Cu(I) ions in the *yz* plane. Cu(I) ions in Cu_2O exist in a linear two-coordinate structure and show a preedge peak at 8982 eV, as shown in Figure 6d. The Cu(II) species exhibited a weak absorption at around 8976−8979 eV, attributed to the dipole-forbidden $1s \rightarrow 3d$ electronic transition, in addition to the shoulder peak at around 8985−8988 eV and an intense peak at around 8995−8998 eV, both attributed to the $1s \rightarrow 4p$ electronic transition. All these features can be recognized in the XANES spectrum of CuO, as shown in Figure 6c. Moreover, Cu(I)Mn−ZSM-5 and Cu(I)−ZSM-5 exhibited a sharp preedge peak at 8983 eV but exhibited no peaks due to the Cu(II) ions at around 8676 eV, indicating that the Cu(II) ions are reduced completely to 2- or 3-coordinated Cu(I) ions after evacuation, as shown in Figures 6a and 6b.[30]

On the other hand, as can be seen in Figure 6, Fourier transforms of the Cu K-edge EXAFS spectra (FT-EXAFS) of the Cu(I)Mn−ZSM-5 and Cu(I)−ZSM-5 catalysts showed a strong peak at around 1.6 Å (no phase-shift correction), which can be ascribed to a backscattering from the first nearest oxygen atoms. Moreover, no peak due to the neighboring copper atoms (Cu−O−Cu) at around 2.6 Å could be observed for these two

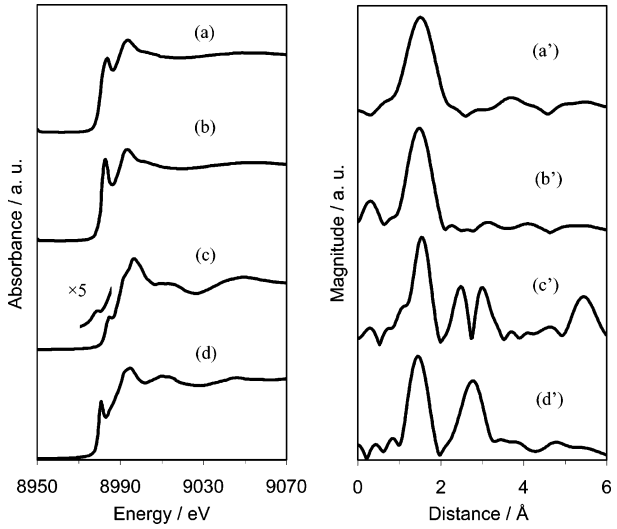

Figure 6. Cu K-edge XANES (left) and FT-EXAFS (right) spectra of (a, a′) Cu(I)Mn−ZSM-5; (b, b′) Cu(I)-ZSM-5; (c, c′) CuO; and (d, d′) Cu_2O. Cu(I)Mn−ZSM-5 and Cu(I)−ZSM-5 were prepared by the evacuation of the as-prepared samples at various temperatures for 1 h. Evacuation temperature: (a) 973 K; (b) 1173 K.

TABLE 3: Results[a] of the Curve-Fitting of the Cu K-Edge EXAFS Spectra for Cu(I)−ZSM-5 and Cu(I)Mn−ZSM-5

samples	shell	CN[b]	R(Å)[c]	σ (Å)[d]
Cu(I)-ZSM-5	Cu−O	2.34	1.86	0.007
Cu(I)Mn−ZSM-5	Cu−O	2.70	1.93	0.007
reference compounds				
CuO	Cu−O	4	1.96	
	Cu−Cu	4	3.00	
Cu_2O	Cu−O	2	1.85	
	Cu−Cu	12	3.02	

[a] Cu(I)Mn−ZSM-5 and Cu(I)−ZSM-5 were prepared by the evacuation of Cu(II)Mn−ZSM-5 at 973 K and Cu(II)−ZSM-5 at 1173 K, respectively, for 1 h. [b] Coordiantion number. [c] Bond distance. [d] Debye−Waller factor

catalysts, indicating that the Cu(I) ions are highly dispersed in ZSM-5 and do not aggregate to form either CuO or Cu_2O clusters. The results of the curve-fitting analysis of the FT-EXAFS spectra are shown in Table 3. Both the Cu−O coordination number (CN) and the Cu−O bond distance (d(Å)) determined for Cu(I)Mn−ZSM-5 (CN = 2.34, d = 1.86 Å) and Cu(I)−ZSM-5 (CN = 2.70, d = 1.93 Å) are in good agreement with those obtained for Cu(I) ions within various zeolites,[28−31] indicating that both 2-coordinate and 3-coordinate Cu(I) ions are present within the zeolite cages, as further supported by results of the XANES measurements.

Photoluminescence Investigations. Due to the high sensitivity of Cu(I) to its environment, photoluminescence spectroscopy has been widely employed in characterization studies of Cu(I) ions in zeolites. Figure 2 shows the photoluminescence spectra of Cu(I)Mn−ZSM-5 and Cu(I)−ZSM-5 measured under vacuum at both 298 K and at 77 K. Two main peaks at 480 and 540 nm can be assigned to the $3d^9 4s^1(^3D_2) \rightarrow 3d^{10}(^1S_0)$ electronic transition of the Cu(I) ions. It should be noted that the emission of Cu(I)Mn−ZSM-5 observed at 540 nm is more intense than that at 480 nm, while the reverse is observed for Cu(I)−ZSM-5. The peak position of the emission of Cu(I) ions reflects the energy difference between the lowest d^9s^1 and d^{10} levels, which is greatly affected by the symmetry of the ligand field of the Cu(I) ion. The two photoluminescence bands observed, thus, indicate that two kinds of Cu(I) ions with different coordination symmetries exist within ZSM-5. The emission bands at 480 and

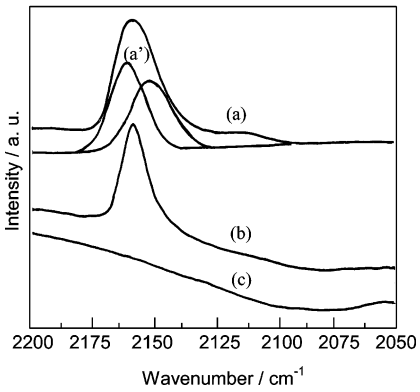

Figure 7. Effect of the evacuation temperature on the FT-IR spectrum of CO adsorbed on Cu(I)Mn−ZSM-5 prepared by the evacuation of Cu(II)Mn−ZSM-5 at 973 K for 1 h. Evacuation temperature: (a) 373 K; (b) 573 K; and (c) 873 K. The two spectra depicted as (a′) are the deconvoluted spectra of (a).

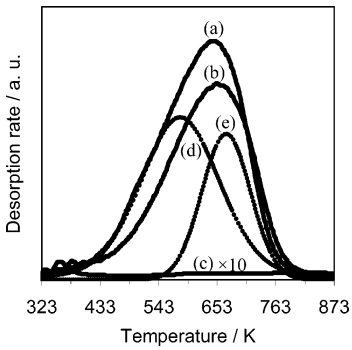

Figure 8. CO−TPD profiles of (a) Cu(I)Mn−ZSM-5; (b) Cu(I)−ZSM-5; (c) Mn−ZSM-5 prepared by the evacuation of the samples at various temperatures for 1 h; and (d, e) the deconvoluted profiles of (a). Evacuation temperature: (a) 973 K; (b) 1173 K; and (c) 973 K.

540 nm can be attributed to the radiative deactivation of 2-coordinate and 3-coordinate Cu(I) ions [$3d^9 4S^1(^1D_2) \rightarrow 3d^{10}(^1S_0)$], respectively, since the 2-coordinate Cu(I) exhibit photoluminescence in shorter wavelength regions than that of the 3-coordinate Cu(I).[32] This assignment is in accordance with a report by Dedecek et al.[33] showing that the emission band at 540 nm corresponds to the isolated Cu(I) ions with C_{3v} symmetry coordinated to the three-framework oxygen atoms of the regular six-membered ring above the oxygen plane. Moreover, it was found that the emission intensity at 480 nm decreased remarkably at 298 K, while the emission intensity at 540 nm was not greatly affected by the temperature of the photoluminescence measurements. Considering that the photocatalytic activity shows a good relationship with the intensity of photoluminescence measured at 298 K, as shown in Figure 4, it can be concluded that the 3-coordinate Cu(I) ions characterized by the emission at 540 nm are the active species for the photocatalytic reaction. These results are also supported by a report by Witchtervola et al.[34] that Cu(I) ions characterized by the photoluminescence band at 540 nm show a correlation between the integrated intensity and the catalytic activity for a thermal NO decomposition reaction.

FT-IR and TPD Investigations. It is generally accepted that CO adsorbs on Cu(I) ions within zeolites to form stable one-on-one carbonyl species (Cu(I)−CO) due to the low charge and high d-electron density of the Cu(I) ions, whereas Cu(II)−CO and Cu(0)−CO are easily decomposed upon evacuation at 298 K. Figure 7 shows the effect of the evacuation temperature on the FT-IR spectrum of CO absorbed on the Cu(I)Mn−ZSM-5 catalyst. The addition of CO onto Cu(I)Mn−ZSM-5 followed by evacuation at 373 K led to the appearance of a band at 2156 cm^{-1} due to the one-on-one Cu(I)-CO complex, as shown in Figure 7a. Cu(I)−ZSM-5 shows a similar spectrum under the same conditions (data not shown). The band at 2156 cm^{-1} has been deconvoluted into two peaks at 2151 and 2159 cm^{-1}, which can be assigned to the CO absorbed on the 3-coordinate and 2-coordinate Cu(I) sites, respectively.[35] Moreover, Brand et al.[36] have reported that $[(H_2O)_2CuCO]^+$ and $[(H_2O)_3CuCO]^+$ complexes exhibit typical FT-IR peaks due to the C−O stretching vibration at 2140 and 2116 cm^{-1}, respectively. These results are also consistent with our assignment that the vibration energy of CO adsorbed on 2-coordinate Cu(I) is higher than that of CO adsorbed on 3-coordinate Cu(I). Further evacuation at 573 K led to a clear decrease in the peak at 2151 cm^{-1}, as shown in Figure 7b. These results indicated that CO desorbed more easily from 3-coordinated Cu(I) (2151 cm^{-1}) than from 2-coordinated Cu(I) (2159 cm^{-1}) during thermovacuum treatment.

Although deconvolution analysis of the IR spectra of the absorbed CO species has made it possible to distinguish the different Cu(I) sites, it is difficult to quantitatively determine the number of Cu(I) ions with different coordination spheres since the CO adsorbed on different Cu(I) sites may have different adsorption coefficients of IR. However, CO-TPD measurements have made it possible not only to distinguish the Cu(I) sites with different coordination spheres but also to determine the relative concentration of these Cu(I) sites, as reported by Nachtigall et al.[37,38]

The CO−TPD profile of Mn−ZSM-5 shows a very weak peak at 353 K, indicating that the interaction between the CO molecules and Mn ions is very weak, as shown in Figure 8. Moreover, no characteristic peak attributed to the CO molecules adsorbed on the Mn ions can be observed in the FT-IR spectra of Cu(I)Mn−ZSM-5, as shown in Figure 7, indicating that no CO−Mn complexes have been formed. These results show that the peaks observed for the CO−TPD profiles of the Cu(I) ion catalysts (Figures 8a,b) can be assigned to the CO desorption from the Cu(I) sites. Both the CO−TPD profiles of Cu(I)Mn−ZSM-5 and Cu(I)−ZSM-5 showed a single broad and asymmetrical peak at temperature regions of 323−823 K, suggesting that the heterogeneity of the Cu(I) sites is responsible for the peak broadness. In fact, these CO−TPD spectra are well-deconvoluted into two bands corresponding to the CO molecules adsorbed on two different kinds of Cu(I) sites, as shown in Figure 8. Band (a) observed at around 573 K (Figure 8d) can be assigned to the CO molecules adsorbed on the 3-coordinate Cu(I) ions while band (b) at higher temperature regions of around 673 K (Figure 8e) can be assigned to those adsorbed on the 2-coordinate Cu(I) ions, as analyzed by results of FT-IR studies. Furthermore, these deconvoluted CO-TPD profiles show a good coincidence with those reported for Cu−ZSM-5 by Nachtigall et al.[38] The relative amounts of CO molecules desorbed from two kinds of Cu(I) ions were determined from the areas of the deconvoluted bands, which were proportional to the amounts of the Cu(I) sites. The area ratio of band (a) to band (b) was determined by the deconvoluted CO−TPD profiles and the results are shown in Table 4. It could, thus, be concluded that the Cu(I)Mn−ZSM-5 catalyst contains larger amounts of 3-coordinate Cu(I) ions as the major Cu(I) moiety than Cu(I)−ZSM-5. The average coordination numbers of Cu(I) ions, calculated on the basis of CO−TPD measurements, show good agreement with those obtained by curve fitting analysis of EXAFS (Table 3), indicating that CO-TPD measurements are

TABLE 4: Results of the Deconvolution of the CO−TPD Spectra and Calculated Coordination Numbers (CN) of Cu(I) Ions Based on the Results of CO−TPD and EXAFS Analyses

catalyst	area ratio (band a/band b)	CN[a] (CO-TPD)	CN (EXAFS)
Cu(I)−ZSM-5	0.863	2.46	2.34
Cu(I)Mn−ZSM-5	1.87	2.65	2.70

[a] Coordination numbers are calculated based on the assumption that the 3-coordinate Cu(I) ions correspond to band (a) while the 2-coordinate Cu(I) ions correspond to band (b), as shown in Figures 8d and 8e.

an effective method in evaluating the relative amounts of Cu(I) moieties with different coordination symmetries.

Since the concentration of 3-coordinate Cu(I) ions present in Cu(I)Mn−ZSM-5 is higher than those in Cu(I)−ZSM5, the strong UV absorption observed in wavelength regions above 250 nm can be attributed to the 3-coordinate Cu(I) ions, as shown in Figure 5. Moreover, Cu(I)Mn−ZSM5 irradiated by UV light at wavelengths above 250 nm shows about 1.8 times higher activity than that of Cu(I)−ZSM5 and about 1.4 times higher activity under irradiation by UV light at wavelengths above 200 nm, as shown in Figure 3. The high photocatalytic activity of Cu(I)Mn−ZSM-5 can be ascribed to the presence of 3-coordinate Cu(I) ions with high concentrations.

Nachtigall et al.[38] have reported that Cu(I) ions at the intersections of the ZSM-5 channels (I2 sites) exhibit higher CO desorption energy (121.8 kJ/mol) than Cu(I) ions at the main channel wall (M7 sites) (96.7 kJ/mol). It could also be concluded that 2-coordinate Cu(I) are coordinated to two oxygen atoms of one AlO_4 tetrahedral at the intersections of the channels (I2 sites), while 3-coordinate Cu(I) ions are coordinated to three oxygen atoms of two AlO_4 tetrahedrals on top of the six-membered rings in the main channel walls (M7 sites), showing good agreement with the results reported by Pietrzyk et al.[39] Nachtigall et al.[40] have also reported that CO adsorption onto the 3-coordinate Cu(I) does not affect its coordinate number; i.e., after CO adsorption, Cu(I) is coordinated by two atoms of the single AlO_4 unit and a carbon atom of CO. On the other hand, CO adsorption onto the 2-coordinate Cu(I) led to changes in the coordination number to 3, coordinated by two framework oxygen and one CO. The drastic changes in the coordination sphere of 3-coordiante Cu(I) explains the small CO adsorption energy, as observed in Figure 7. Nactigallova et al.[41] have further investigated the coordination changes on the reduction of Cu(II) ions into Cu(I) in ZSM-5 by combined quantum mechanic/interatomic potential function techniques, suggesting that Cu(II) ions at the zigzag channels (Z5 sites) are transferred to the channel intersections and reduced into 2-coordinate Cu(I) ions.[42] It could, thus, be reasonably concluded that Cu(II) $_\alpha$ ions at the main channels (M7 sites) are reduced to 3-coordinated Cu(I) ions at the M7 sites, as characterized by the photoluminescence at 540 nm. On the other hand, Cu(II) $_\beta$ ions at the Z5 sites are easily reduced to 2-coordinate Cu(I) ions at the I2 sites, as identified by the photoluminescence at 480 nm.

The pre-ion-exchanged Mn ions, thus, preferentially occupy the Z5 sites and induce more Cu(II) ions to be exchanged at the six-membered rings in the main channels to form a square pyramidal coordination. This led to a lesser population of Cu(II) ions with a distorted square pyramidal coordination located in the zigzag channels, as evidenced by ESR measurements (Figure 1). After evacuation at high temperatures, the Cu(II) ions located at the six-membered rings in the main channels were selectively reduced into 3-coordinate Cu(I) ions on top of the six-membered rings in the main channel walls, while the Cu(II) ions located in the zigzag channels were transferred to the channel intersections and reduced into 2-coordinate Cu(I) ions. The higher concentration of 3-coordinate Cu(I) ions in Cu(I)Mn−ZSM-5 than in Cu(I)−ZSM-5 was confirmed by photoluminescence, UV−vis, XAFS, and TPD analyses. The introduction of Mn ions into Cu(I)−ZSM-5 was, thus, seen to cause more 3-coordinate Cu(I) ions to be present in the main channels of ZSM-5, leading to high photocatalytic activity for the decomposition of N_2O into N_2 and O_2. These results demonstrated that pre-ion-exchange with Mn ions is an easy and effective method in enhancing the photocatalytic activity of Cu(I) ion catalysts within ZSM-5 zeolites.

Conclusions

Cu(I)Mn−ZSM-5 prepared by a combination technique of ion-exchange and evacuation at high temperatures was found to show higher activity than Cu(I)−ZSM-5 for the direct photocatalytic decomposition of N_2O into N_2 and O_2 under UV light irradiation at 298 K.

ESR investigations revealed that the introduction of Mn ions into ZSM-5 induced the preferential exchange of Cu(II) ions at the main channels of the zeolite, i.e., M7 sites, during the ion-exchange process. It was also found that the presence of Mn ions accelerated the reduction of Cu(II) ions into Cu(I) during evacuation at high temperatures. A combination of FT-IR and CO−TPD investigations provided an effective evaluation method to determine the relative amounts of the two different kinds of Cu(I) ion species of 2-coordination and 3-coordination symmetry, and these results could be confirmed by XAFS analysis. Spectroscopic measurements clearly showed that the Cu(II) ions at the main channels of Cu(II)Mn−ZSM-5 were selectively reduced into 3-coordinate Cu(I) ions at the M7 sites, playing an major role as the active species for the photocatalytic decomposition of N_2O into N_2 and O_2 at 298 K.

Supporting Information Available: Definitions of the individual Cu sites and their locations in the ZSM-5 framework. This material is available free of charge via the Internet at http://pubs.acs.org.

References and Notes

(1) Iwamoto, M.; Furukawa, H.; Mine, Y.; Uemura, F.; Mikuriya, S. I.; kagawa, S. *J. Chem. Soc., Chem. Commun.* **1986**, 1272.
(2) Anpo, M.; Che, M. *Adv. Catal.* **2000**, *44*, 119.
(3) Matsuoka, M.; Anpo, M. *J. Photochem. Photobiol. C*, **2003**, *3*, 225.
(4) Anpo, M. *Bull. Chem. Soc. Jpn.* **2004**, *77*, 1427.
(5) Chen, H. J.; Matsuoka, M.; Zhang, J. L.; Anpo, M. *J. Catal.* **2004**, *228*, 75.
(6) Chen, H. J.; Matsuoka, M.; Zhang, J. L.; Anpo, M. *Chem. Lett.* **2004**, *33*, 1254.
(7) Matsuoka, M.; Anpo, M. *Curr. Opin. Solid State Mater. Sci.* **2003**, *7*, 451.
(8) Anpo, M.; Matsuoka, M.; Hanou, K.; Mishima, H.; Yamashita, H.; Patterson, H. H. *Coord. Chem. Rev.* **1998**, *171*, 175.
(9) Yamashita, H.; Matsuoka, M.; Tsuji, K.; Shioya, Y.; Anpo, M.; Che, M. *J. Phys. Chem.* **1996**, *100*, 397.
(10) Anpo, M.; Matsuoka, M.; Shioya, Y.; Yamashita, H.; Giamello, E.; Morterra, C.; Che, M.; Patterson, H. H.; Webber, S.; Ouellette, S.; Fox, M. A. *J. Phys. Chem.* **1994**, *98*, 5744.
(11) Iwamoto, M.; Yokoo, S.; Sakai, K.; Kagawa, S. *J. Chem. Soc., Faraday Trans.* **1981**, *77*, 1629.
(12) Zhang, Y.; Flytzani-Stephanopoulos, M. in: *Environmental Catalysis*; J. N. Armor, Ed.; American Chemical Society: Washington, DC, 1994; p 7.
(13) Budi, P.; Curryhyde, E.; Howe, R. F. *Catal. Lett.* **1996**, *41*, 47.
(14) Kucherov, A. V.; Hubbard, C. P.; Kucherova, T. N.; Shelef, M. Progress in zeolite and microporous materials. In Studies in Surface Science

Catalysis; Chon, H.; Ihm, S. K.; Uh, Y. S., Eds.; Elsevier: Amsterdam, 1997; Vol. 105, p 1469.
(15) Parvulescu, V. I.; Centeno, M. A.; Grange, P.; Delmon, B. *J. Catal*. **2000**, *191*, 445.
(16) Zhang, Y.; Flytzani-Stephanopoulos, M. *J. Catal*. **1996**, *164*, 131.
(17) Centi, G.; Perathoner, S. *Appl. Catal. A* **1995**, *132*, 179.
(18) Parvulescu, V. I.; Grange, P.; Delmon, B. *Appl. Catal. B* **2001**, 33, 223.
(19) Kucherov, A. V.; Slinkin, A. A. *Zeolites* **1986**, *6*, 175.
(20) Slinkin, A. A.; Kucherov, A. V.; Chuvylkin, N. D.; Korsunov, V. A.; Kliachko, A. L.; Nikishenko, S. B. *J. Chem. Soc., Faraday Trans. 1* **1989**, 85, 3233.
(21) Levi, Z.; Raitsimring, A. M.; Goldfarb, D. *J. Phys. Chem*. **1991**, *95*, 7830.
(22) Zhang, Q.; Wang, Y.; Itsuki, S.; Shishido, T.; Takehira, K. *J. Mol. Catal. A* **2002**, *188*, 189.
(23) Bentrup, U.; Bruchner, A.; Richter, M.; Fricke, R. *Appl. Catal. B* **2001**, *32*, 229.
(24) Wilkinson, S. G. *Comprehensive coordination chemistry*, 1st ed.; Pergamon Press: New York, 1987; Vol. 1.
(25) Texter, J.; Strome, D. H.; Herman, R. G.; Klier, K. *J. Phys. Chem*. **1977**, *81*, 333.
(26) Tranquada, J. M.; Heald, S. M.; Moodenbaugh, A. R. *Phys. Rev. B*, **1987**, *36*, 5263.
(27) Brown, J. M.; Powers, L.; Kincaid, B.; Larrabee, J. A.; Spirp, T. G. *J. Am. Chem. Soc*. **1980**, *102*, 4210.
(28) Lamberti, C.; Bordiga, S.; Salvalaggio, M.; Spoto, G.; Zecchina, A.; Geobaldo, F.; Vlaic, G.; Bellatreccia, M. *J. Phys. Chem. B* **1997**, *101*, 344.
(29) Groothaert, M. H.; van Bokhoven, J. A.; Battiston, A. A.; Weckhuysen, B. M.; Schoonheydt, R. A. *J. Am. Chem. Soc*. **2003**, *125*, 7629.
(30) Kau, L. S.; Spira-Solomon, D. J.; Penner-Hahn, J. E.; Hodgson, K. O.; Solomon, E. I. *J. Am. Chem. Soc*. **1987**, *109*, 6433.
(31) Kuroda, Y.; Yagi, K.; Hiroguchi, N.; Yoshikawa, Y.; Kumashiro, R.; Nagao, M. *Phys. Chem. Chem. Phys*. **2003**, *5*, 3318.
(32) Matsuoka, M.; Ju, W. S.; Takahashi, K.; Yamashita, H.; Anpo, M. *J. Phys. Chem. B* **2000**, *104*, 4911.
(33) Dedecek, J.; Wichterlova, B.; Kubat, P. *Microporous Mesoporous Mater*. **1999**, *32*, 63.
(34) Dedecek, J.; Wichterlova, B. *Phys. Chem. Chem. Phys*. **1999**, *1*, 629.
(35) Kumashiro, R.; Yoshikawa, Y.; Nagao, M. *J. Phys. Chem. B* **1999**, *103*, 89.
(36) Brand, H. V.; Redondo, A.; Hay, P. J. *J. Phys. Chem. B* **1997**, *101*, 7691.
(37) Davidova, M.; Nachtigallova, D.; Bulanek, R.; Nachtigall, P. *J. Phys. Chem. B* **2003**, *107*, 2327.
(38) Bulanek, R.; Cicmanec, P.; Knotek, P.; Nachtigallova, D.; Nachtigall, P. *Phys. Chem. Chem. Phys*. **2004**, *6*, 2003.
(39) Pietrzyk, P.; Piskorz, W.; Sojka, Z.; Broclawik, E. *J. Phys. Chem. B* **2003**, *107*, 6105.
(40) Davidova, M.; Nachtigallova, D.; Bulanek, R.; Nachtigall, P, *J. Phys. Chem. B* **2003**, *107*, 2327.
(41) Natchigallova, D.; Nachtigall, P.; Sauer, J. *Phys. Chem. Chem. Phys*. **2001**, *3*, 1552.
(42) Nachtigall, P.; Nachtigallova, D.; Sauer, J. *J. Phys. Chem. B* **2000**, *104*, 1738.